From Preceramic Polymers with Interpenetrating Networks to SiC/MC Nanocomposites

Robert J. P. Corriu, Philippe Gerbier,* Christian Guérin,* and Bernard Henner

U.M.R. 5637 Chimie Moléculaire et Organisation du Solide, Université Montpellier II, Sciences et Techniques du Languedoc, Place Eugène Bataillon - Case 007, 34095 Montpellier Cedex 5, France

Received September 6, 1999. Revised Manuscript Received December 2, 1999

The preparation of β-SiC/MC (M = Ti, Nb, and Ta) nanocomposite ceramics by the pyrolysis under an inert atmosphere of precursors consisting in interpenetrating networks of poly[(dimethylsilylene)diacetylene], **1**, and polymeric metal oxide is described. The precursors are obtained by in-situ precipitation of the desired metal alkoxide into the organosilicon polymeric matrix. The precursor-to-ceramic conversion involved two critical transformations: (i) the thermal cross-linking of **1** and (ii) the carbothermal reduction of the oxide by the free carbon resulting from the degradation of **1**. At 1400 °C, the pure carbides are obtained as nanometer-sized highly crystalline powders. Analyses have shown that both β-SiC and the other metal carbide are present simultaneously in each ceramic particle as discrete phases. All of these results show that we are faced with materials that can be described as nanocomposite ceramics with interpenetrating networks.

Introduction

Today's highly technical applications have drastically increased the property requirements demanded of ceramics. As a consequence, new and alternative techniques for the preparation of ceramics have been envisioned. Among them, the pyrolysis of organometallic polymeric precursors that contain structural elements that are desired in the final material has attracted much attention.[1−15] This method offers several unique advantages as compared to traditional powder processing techniques including lower processing temperatures, improved impurity control, and the ability to form near net complex shapes.[16,17] Moreover, this method had proved to be an excellent alternative route for the synthesis of nanocomposite ceramics, which are known to exhibit significantly improved mechanical properties when compared to the isolated phases.[18−24] As an example, high-temperature mechanical improvements of silicon carbide fibers were successful through modification of polycarbosilane polymers with metal alkoxides.[18,19] Modifications of this type enabled the formation of various β-SiC/MC nanocomposite ceramics that might be useful for cutting tools, abrasives, or high-temperature structural applications.

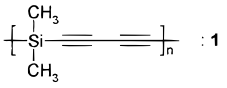

: **1**

In previous works,[25−28] we have described a novel class of organosilicon linear polymers incorporating diacetylenic units such as poly[(dimethylsilylene)diacetylene], **1**. When pyrolyzed at 1400 °C under an argon flow, **1** leads to nanocrystalline β-SiC (size range

* E-mail: gerbier@crit.univ-montp2.fr.

(1) Riedel, R.; Kroke, E.; Greiner, A.; Gabriel, A. O.; Ruwisch, L.; Nicolich, J. *Chem. Mater.* **1998**, *10*, 2964.
(2) Dutremez, S.; Gerbier, Ph.; Guerin, C.; Henner, B.; Merle, Ph. *Adv. Mater.* **1998**, *10*, 465.
(3) Itoh, M.; Inoue, K.; Iwata, K.; Ishikawa, J.; Takenaka, Y. *Adv. Mater.* **1997**, *9*, 1187.
(4) Riedel, R.; Dressler, W. *Ceramics Int.* **1996**, *22*, 233.
(5) Interrante, L. V.; Liu, Q.; Shen, Q. *J. Organomet. Chem.* **1996**, *521*, 1.
(6) Bacqué, E.; Birot, M.; Pillot, J. P.; Lapouyade, P.; Gerval, P.; Biran, C.; Dunoguès, J. *J. Organomet. Chem.* **1996**, *521*, 99.
(7) Birot, M.; Pillot, J.-P.; Dunoguès, J. *Chem. Rev.* **1995**, *95*, 1443.
(8) Bill, J.; Aldinger, F. *Adv. Mater.* **1995**, *7*, 775.
(9) Riedel, R. *Naturwissenschaften* **1995**, *82*, 12.
(10) Corriu, R. J. P.; Enders, M.; Huille, S.; Moreau, J. J. E. *Chem. Mater.* **1994**, *6*, 15.
(11) Paine, R. T.; Janik, J. F.; Fan, M. *Polyhedron* **1994**, *13*, 1225.
(12) Laine, R. M.; Baboneau, F. *Chem. Mater.* **1993**, *5*, 260.
(13) Stanley, D. R.; Birchall, D. J.; Hyland, J. N. K.; Thomas, L.; Hodgetts, K. *J. Mater. Chem.* **1992**, *2*, 149.
(14) Schmidt, W. R.; Interrante, L. V.; Doremus, R. H.; Trout, T. K.; Marchetti, P. S.; Maciel, G. E. *Chem. Mater.* **1991**, *3*, 257.
(15) Boury, B.; Carpenter, L.; Corriu, R. J. P.; Mutin, H. *New J. Chem.* **1990**, *14*, 535.
(16) Greil, P. *J. Eur. Ceram. Soc.* **1998**, *18*, 1905.
(17) Seyferth, D.; Czubarow, P. *Chem. Mater.* **1994**, *6*, 10.
(18) Yajima, S.; Iwai, T.; Yamamura, T.; Okamura, K.; Hasegawa, Y. *J. Mater. Sci.* **1981**, *16*, 1349.
(19) Thorne, K.; Liimatta, E.; Mackenzie, J. D. *J. Mater. Res.* **1991**, *6*, 2199.
(20) Seyferth, D.; Bryson, N.; Workman, D. P.; Sobon, C. A. *J. Am. Ceram. Soc.* **1991**, *74*, 2687.
(21) Seyferth, D.; Lang, H.; Sobon, C. A.; Borm, J.; Tracy, H. J.; Bryson, N. *J. Inorg. Organomet. Polym.* **1992**, *2*, 59.
(22) Jalowiecki, A.; Bill, J.; Friess, M.; Mayer, J.; Aldinger, F.; Riedel, R. *Nanostruct. Mater.* **1995**, *6*, 279.
(23) Chae, K. W.; Niihara, K.; Kim, D.-Y. *J. Mater. Sci. Lett.* **1995**, *14*, 1332.
(24) Dressler, A.; Greiner, A.; Seher, M.; Riedel, R. *Nanostruct. Mater.* **1995**, *6*, 481.
(25) Corriu, R. J. P.; Guérin, C.; Henner, B.; Jean, A.; Mutin, H. *J. Organomet. Chem.* **1990**, *396*, C35.
(26) Corriu, R. J. P.; Gerbier, Ph.; Guérin, C.; Henner, B.; Jean, A.; Mutin, H. *Organometallics* **1992**, *11*, 2507.
(27) Corriu, R. J. P.; Gerbier, Ph.; Guérin, C.; Henner, B.; Fourcade, R. *J. Organomet. Chem.* **1993**, *449*, 111.
(28) Bréfort, J. L.; Corriu, R. J. P.; Gerbier, Ph.; Guérin, C.; Henner, B.; Jean, A.; Kuhlmann, Th.; Garnier, F.; Yassar, A. *Organometallics* **1992**, *11*, 2500.

10.1021/cm991140e CCC: $19.00
Published on Web 02/12/2000

= 2.5−5 nm) regularly dispersed into an amorphous carbon matrix with a formula of SiC-4C. The exothermic cross-linking of the diacetylenic units that occurs in the solid state at 200 °C, overcomes depolymerization processes and explains the high ceramic yield obtained for a linear polymer.[25−27,29] These properties led us to prepare β-SiC/metal carbide (or nitride) precursors by dispersing a metal oxide in polymer **1**.[30,31] The metal oxide:**1** ratio is adjusted in such a way that the carbothermal consumption of the excess of carbon by the oxide provides pure β-SiC/metal carbide (or nitride) ceramics.

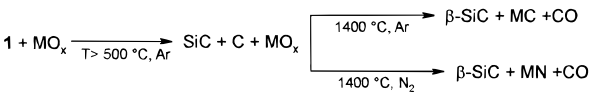

As compared to the traditional solid-state reactions, this approach provides an intimate mixture of the metal oxides particles and the preceramic polymer reactive matrix. For that reason, the carbothermal reduction occurs with improved kinetics and at temperatures lower than those reported for the conventional methods. The final ceramic consists of particles constituted by an agglomerate of crystals of both β-SiC and the metal carbide or nitride. Because the interpenetration of the phase domains depends on the size and shape of the starting metal oxide particles, an improvement may be obtained by using a molecular precursor to the metal oxide. Previously, the reaction between a metal alkoxide and Yajima's polycarbosilane has been described.[18,19] This reaction results in the formation of a modified polymer that can be converted thermally into binary ceramics of SiC and the corresponding metal carbide. These developments suggested to us that a β-SiC/MC nanocomposite precursor might be obtained by dispersing a metal oxide source, such as metal alkoxide, in **1**. This paper reports the synthesis of β-SiC/TiC, β-SiC/NbC, and β-SiC/TaC nanocomposites starting from precursors consisting in interpenetrating networks of poly[(dimethylsilylene)diacetylene] and polymeric metal oxides.

Experimental Section

Materials. Ti(OPr^i)$_4$, Nb(OEt)$_5$, and Ta(OEt)$_5$ were purchased from Aldrich and used as received. THF was distilled over CaH_2 before use. Argon (ultrapure grade) was purchased from L'Air Liquide and used without further purification. **1** was prepared according to the procedure published previously.[28]

Instrumentation. All pyrolyses were performed in a Carbolite alumina tube furnace fitted with taps to allow the connection to a vacuum line. Powder X-ray diffraction (XRD) patterns were recorded on a Philips diffractometer using Cu Kα radiation. Transmission electron microscopy (TEM) coupled with energy dispersive analysis of X-ray (EDX) were carried out on a Philips CM 20 microscope operating at 200 kV equipped with a TRACOR microprobe. Powder specimens were suspended in ethanol and spread onto a copper grid recovered with an amorphous carbon film. Thermal analyses were carried out with a Netzsch STA 409 thermogravimetric analyzer coupled to a Balzers QMG 421 mass spectrometer. Thermogravimetric analyses (TGA) were recorded in the range 20−1400 °C under argon flow (60 mL min^{-1}) at a heating rate of 10 °C min^{-1}. Differential scanning calorimetric (DSC) experiment were conducted on a Mettler 30 instrument. Specific surface-area measurements (BET method) were carried out on a Micromeritics Pulse Chemisorb 2700 operating with a helium−nitrogen mixture (70:30). IR spectra were taken on a Perkin-Elmer 1600 FT either in KBr pellets or in Nujol mulls. Elemental analyses were performed at the Service Central de Microanalyse of the CNRS, Vernaison, France.

Table 1. Precursors Preparation

precursor	metal alkoxide	**1** [g] (equiv.)	metal alkoxide [g] (equiv.)	initial Si:M:C ratio
2	Ti(OPr^i)$_4$	0.28 (3)	1.00 (4)	3:4:15
3	Nb(OEt)$_5$	0.29 (7)	1.00 (8)	7:8:35
4	Ta(OEt)$_5$	0.27 (7)	1.00 (8)	7:8:35

Precursor Preparation. The procedure is similar for all the composites described therein. In the first step, appropriate quantities of **1** and metal alkoxide (Table 1) were dissolved in THF. The mixture was left for 5 min under stirring, and the solvent was evaporated under reduced pressure to yield a waxy residue. The residue was transferred onto an open dish and placed in a ventilated oven at 60 °C for 24 h in order to hydrolyze the metal alkoxide by the ambient moisture. The resulting orange-beige solid was then ground into a powder, and the remaining alcohol molecules resulting from the hydrolysis were removed under vacuum.

Pyrolysis. A sample of precursor was weighed in an alumina crucible and placed into the tube furnace. After three argon purges, the sample was heated at 5 °C min^{-1} to 250 °C and then at 10 °C min^{-1} to 1400 °C under a continuous flow of argon (90 mL min^{-1}). The final temperature was maintained for 2.5 h before being allowed to cool to room temperature. The pyrolysis yielded the nanocomposite ceramics as black ultrafine powders. Anal. for SiC/TiC: found $Ti_{4.00}Si_{2.71}C_{7.10}$, expected $Ti_{4.00}Si_{3.00}C_{7.00}$. Anal. for SiC/NbC: found $Nb_{8.00}Si_{6.95}C_{15.80}$, expected $Nb_{8.00}Si_{7.00}C_{15.00}$. Anal. for SiC/TaC: found $Ta_{8.00}Si_{6.80}C_{15.13}$, expected $Ta_{8.00}Si_{7.00}C_{15.00}$.

Results and Discussion

Precursors Synthesis and Characterization. The metal alkoxide/polymer precursors were prepared by adding the appropriate metal alkoxide to a THF solution of **1**, followed by vacuum evaporation of the solvent. The molar ratio of **1**:metal alkoxide was based on the following transformations (eqs 1−4):

$$\mathbf{1} \xrightarrow[\Delta,\ Ar]{} SiC + 4C + H_2 + CH_4 \qquad (1)$$

$$M(OR)_x \xrightarrow[H_2O]{} MO_{x/2} + x\mathrm{ROH} \qquad (2)$$

$$MO_{x/2} + (x/2 + 1)C \xrightarrow[\Delta,\ Ar]{} MC + (x/2)CO \qquad (3)$$

$$(x/2 + 1)\mathbf{1} + 4M(OR)_x \xrightarrow[2)\ \Delta,\ Ar]{1)\ \text{hydrol.}} (x/2 + 1)SiC + 4MC + ... \qquad (4)$$

The resulting moisture-sensitive mixtures were submitted to the atmosphere in a ventilated oven at 60 °C, followed by a vacuum treatment to yield beige powders, **2**−**4**. This step was shown to be crucial to avoid the thermal volatilization of the metal alkoxide entrapped inside the polymer matrix during the pyrolysis. The infrared spectrum of a precursor **2** originated from a Ti(OPr^i)$_4$/**1** mixture treated under the above conditions is shown in Figure 1. The absence of the characteristic

(29) Kuroki, S.; Okita, K.; Kakigano, T.; Ishikawa, J.; Itoh, M. *Macromolecules* **1998**, *31*, 2804.
(30) Corriu, R. J. P.; Gerbier, Ph.; Guérin, C.; Henner, B. *Angew. Chem., Int. Ed. Eng.* **1992**, *31*, 1195.
(31) Corriu, R. J. P.; Gerbier, Ph.; Guérin, C.; Henner, B. *Adv. Mater.* **1993**, *5*, 380.

Table 2. Stoichiometry of the Precursors and Ceramic Results

precursor	stoichiometry of the precursor	ceramic yield [%]	M/Si[a] ratio ()[b]	phases identified by XRD
2	3 **1** + 4 Ti[(O_{2-X}) OH_{2X}]·y H_2O	39	1.5 ± 0.2 (1.3)	β-SiC + TiC
3	7 **1** + 4 Nb_2O[(O_{4-X}) OH_{2X}]·y H_2O	51	1.1 ± 0.2 (1.1)	β-SiC + NbC
4	7 **1** + 4 Ta_2O[(O_{4-X}) OH_{2X}]·y H_2O	60	1.1 ± 0.2 (1.1)	β-SiC + TaC

[a] Determined by EDX. [b] Numbers in parentheses are the theoretical M/Si ratio.

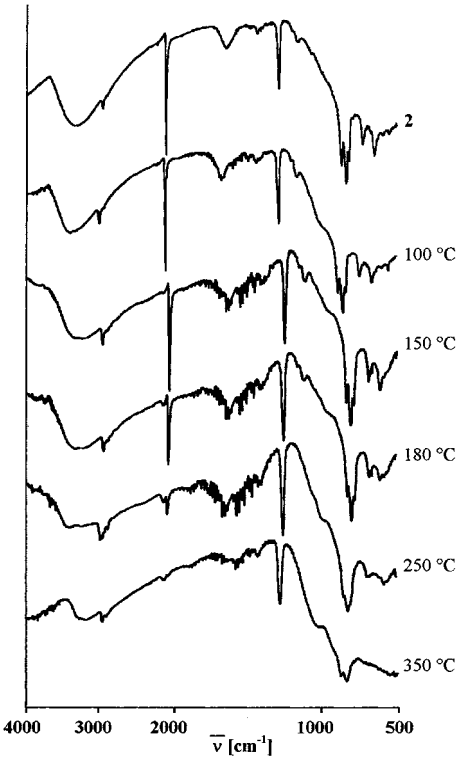

Figure 1. Infrared spectra (KBr pellets) of precursor **2** heated at various temperatures.

vibrations corresponding to the Pr^i groups (2932, 2867 $cm^{-1} = \nu_{CH}$; 1376, 1355 $cm^{-1} = \delta_{Pr^i}$) indicates that the complete hydrolysis of the metal alkoxide has occurred. Moreover, the strong, broad absorption centered at 3347 cm^{-1}, associated with the one at 1630 cm^{-1}, suggests that the titanium oxide can be described by the empirical formula Ti[$(O_{2-x})OH_{2x}$]·y H_2O.

To isolate and characterize the inorganic moiety from the precursor, **2** was washed with THF and the resultant suspension centrifuged to yield a white precipitate that was identified as Ti[$(O_{2-x})OH_{2x}$]·$y H_2O$. The TEM micrograph of the precipitate (Figure 2a) showed a spongelike solid constituted by an entanglement of nanometer-sized filaments.

The comparison with a titanium oxide colloid obtained from the slow hydrolysis of an ethereal solution of $Ti(OPr^i)_4$ (Figure 2b) showed quite different particle size and morphology. These differences may be related to the growth of organic−inorganic composite materials by chemical precipitation of particles in a polymer matrix.[32] This approach, which is built on an analogy with biological mineralization, allows the control of both the particles size and shape to form the complex nanostructures observed in Figure 2a.[32] In agreement with these observations and the literature,[33] the precursors described here may be described as organometallic−inorganic nanocomposites with interpenetrating networks.

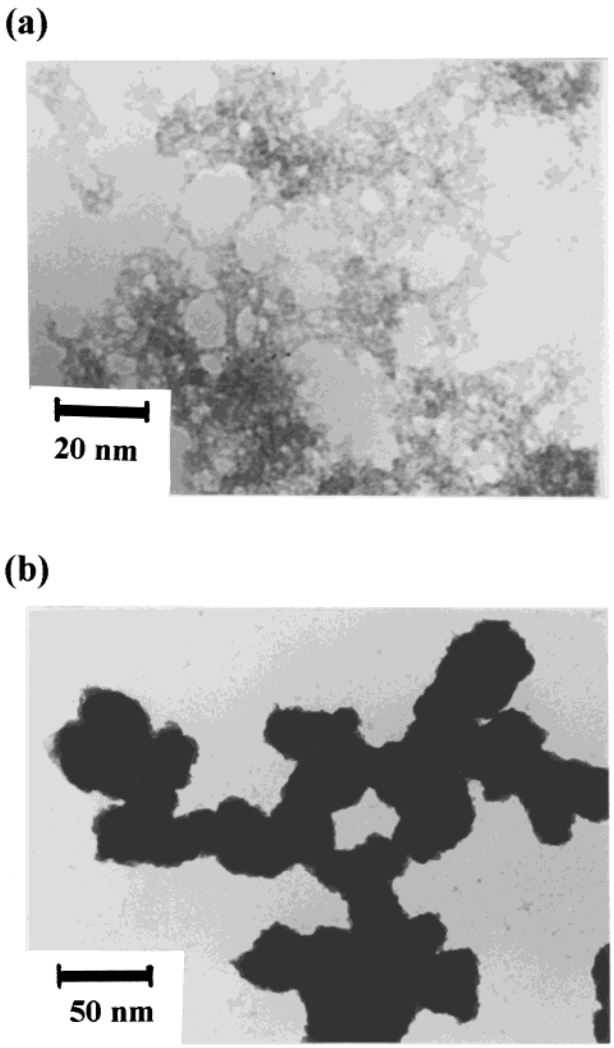

Figure 2. TEM micrographs of titanium oxide particles precipitated from (a) **2** and (b) an ethereal solution of $Ti(OPr^i)_4$.

Precursor Pyrolysis. The pyrolysis of the precursors up to 1400 °C for 2 h under argon produced ultrafine black powders in good ceramic yields. EDX analysis exhibited a M/Si ratio close to the ratio present in the starting precursor (Table 2). Figures 3e, 4e, and 5e show the XRD patterns of the resulting ceramics. In each case, β-SiC and the corresponding metal carbide (TiC, NbC, and TaC) were identified as the only crystalline phases.[34] The cell parameter of the metal carbides clearly indicated the total conversion of the initial metal oxide into its corresponding carbide. The IR spectra

(32) Calvert, P. D.; Broad, R. A. *Contemp. Topics Polym. Sci.* **1986**, *6*, 95.

(33) Jackson, C. L.; Bauer, B. J.; Nakatani, A. I.; Barnes, J. D. *Chem. Mater.* **1996**, *8*, 727.

(34) Phases identified according to the following *JCPDS* file Nos.: 29-1129 (β-SiC); 27-605 (α-SiO_2); 32-1383 (TiC); 10-63 (Ti_2O_3); 11-217 and 23-606 (Ti_3O_5); 38-1363 (NbC); 34-898 (NbO_2); 35-801 (TaC); 19-1294 (ζ-$TaC_{0.6}$); 18-1304 (δ-Ta_2O_5); 19-1299 (δ-(Ta, O)).

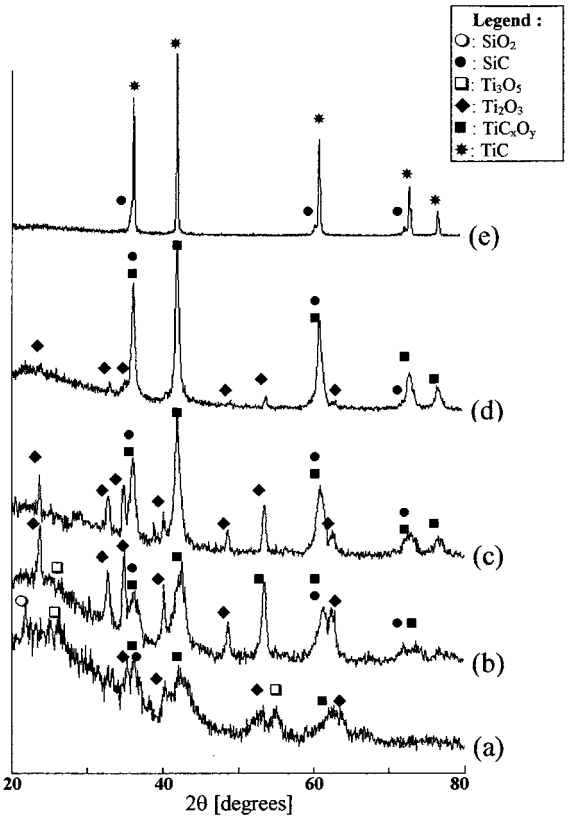

Figure 3. X-ray diffraction patterns of **2** heated to (a) 1000 °C for 10 min, (b) 1200 °C for 10 min, (c) 1300 °C for 10 min, (d) 1400 °C for 10 min, and (e) 1400 °C for 1 h.

(Figure 6) revealed only the characteristic absorption of SiC at about 820 cm^{-1}. No absorption that could be assigned to unreacted oxide-based amorphous phases can be found in the 450−1100 cm^{-1} region.[35,36]

As determined by TEM, the grain sizes and microstructure of the β-SiC/metal carbide ceramics were found to depend on the nature of the metal (Figure 7). The sample of SiC/TiC (Figure 7a) is constituted of loosely aggregated rounded crystallites from which the particle size analysis showed a rather sharp distribution centered at 20 nm. The SiC and TiC phases distribution was investigated by selected area electron diffraction (SAED)−EDX analysis of sets of 2−5 nanoparticles. SAED showed only punctuated diffraction rings attributed to pure TiC. Likely because of the cell parameter similarities between β-SiC and TiC, the diffraction rings associated with β-SiC are not observed by SAED. Nevertheless, the EDX spectra showed that Si and Ti were present simultaneously within each set of particles and that the Si/Ti ratio was found to be homogeneous for all the analyses. Consistent with these results and the observed coexistence of Si(C) and Ti(C) in some larger isolated particles, it can be assumed first that both the β-SiC and TiC phases are simultaneously present in each nanoparticle and second that both of the components are present in similar ratios. According to the classification of the nanocomposites suggested by Niihara,[37] the SiC/TiC ceramic described here may be considered as belonging to the nano/nano type.

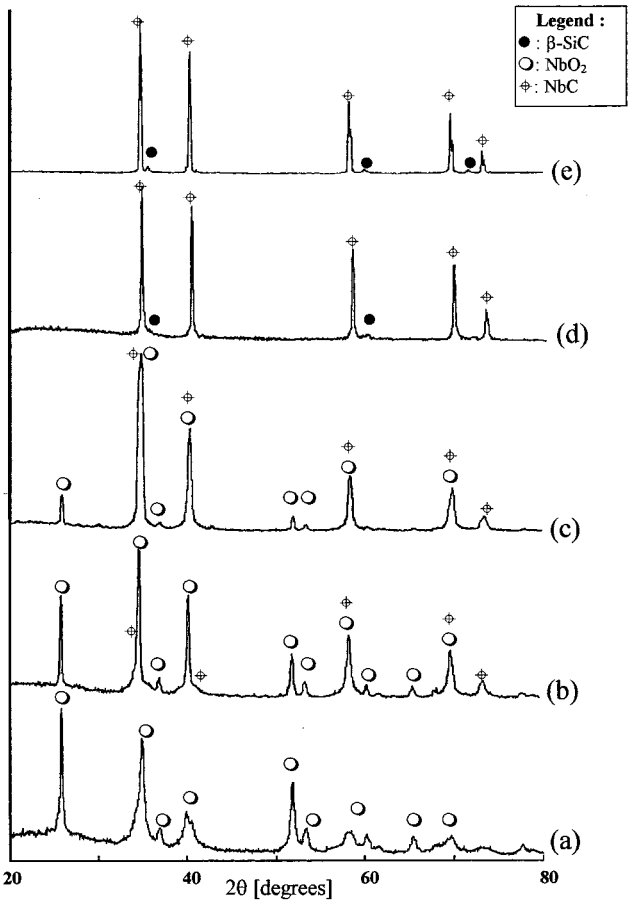

Figure 4. X-ray diffraction patterns of **3** heated to (a) 1000 °C for 10 min, (b) 1200 °C for 10 min, (c) 1300 °C for 10 min, (d) 1400 °C for 10 min, and (e) 1400 °C for 1 h.

Compared to SiC/TiC, the TEM micrographs of SiC/NbC or of SiC/TaC samples (Figure 7b,c, respectively) showed significant grain morphology and microstructure differences. The materials were constituted of elongated particles with an approximate section of 30 × 30 nm^2, in which faceted crystallites of 5−30 nm in size were embedded. SAED−EDX analyses indicated that the faceted crystallites were constituted of pure NbC or TaC, respectively, whereas the elongated body of the particles was formed of SiC. Surface area BET measurements have been carried out on these samples. As expected from the TEM observations, the specific surface area of the SiC/TiC ceramic (416 $m^2\ g^{-1}$) differs appreciably from those of the SiC/NbC (225 $m^2\ g^{-1}$) and the SiC/TaC (187 $m^2\ g^{-1}$) ceramics. These very high values, in comparison to those reported for the ceramics prepared from traditional solid-state techniques, are often reported with materials originated from organometallic precursors, and reflects the extremely small particle size of our SiC/metal carbide composites.[38]

The precursor-to-ceramic conversion processes were followed by the TGA-MS method. As illustrated for the precursor **2** (Figure 8), three weight losses were observed during the pyrolysis. The initial two-step weight loss, consistent with the dehydration of the inorganic moiety and the polymer decomposition, occurred in the 50−750 °C range for each sample and was found to be slightly dependent upon the nature of the metal. The

(35) Ramis, G.; Quintard, P.; Cauchetier, M.; Busca, G.; Lorenzelli, V. *J. Am. Ceram. Soc.* **1989**, *72*, 1692.
(36) McDevitt, N. T.; Baun, W. L. *Spectrochim. Acta* **1964**, *20*, 799.
(37) Niihara, K. *J. Ceram. Soc. Jpn.* **1991**, *99*, 974.
(38) Chorley, R. W.; Lednor, P. W. *Adv. Mater.* **1991**, *10*, 474.

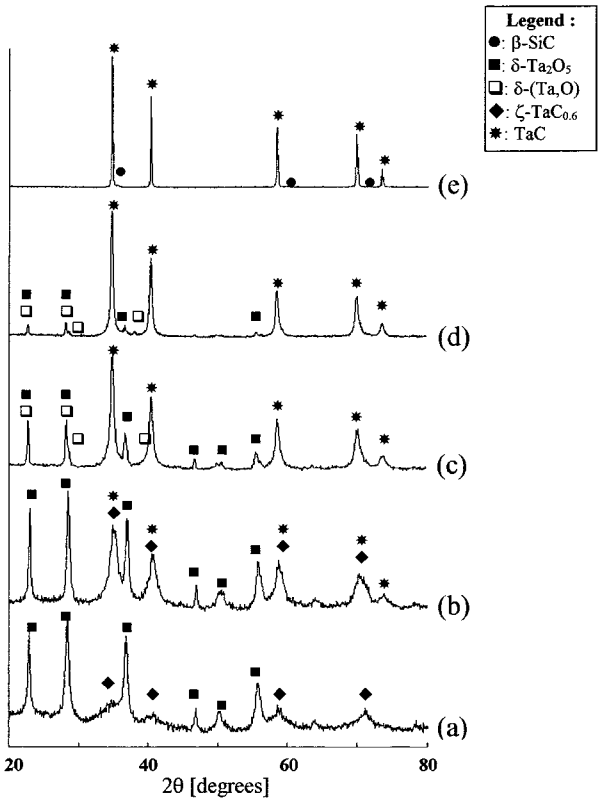

Figure 5. X-ray diffraction patterns of **4** heated to (a) 1000 °C for 10 min, (b) 1200 °C for 10 min, (c) 1300 °C for 10 min, (d) 1400 °C for 10 min, and (e) 1400 °C for 1 h.

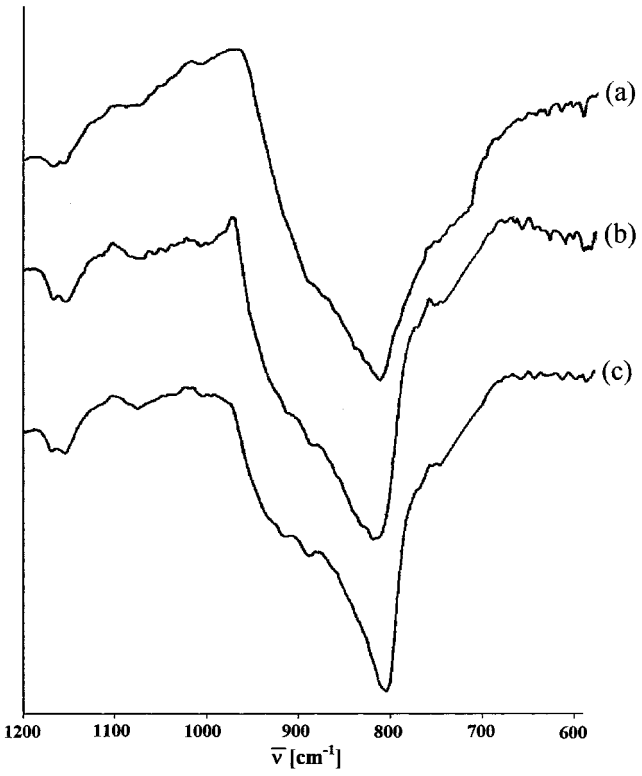

Figure 6. Infrared spectra (Nujol mulls) of the (a) SiC/TiC, (b) SiC/NbC, and (c) SiC/TaC ceramics heated to 1400 °C for 2 h.

broad endotherm that was observed in the DSC curve near 100 °C (Figure 9a) was assigned to the dehydration process, whereas the broad exotherm at the end of the first weight loss (ca. 200 °C) was attributed to the

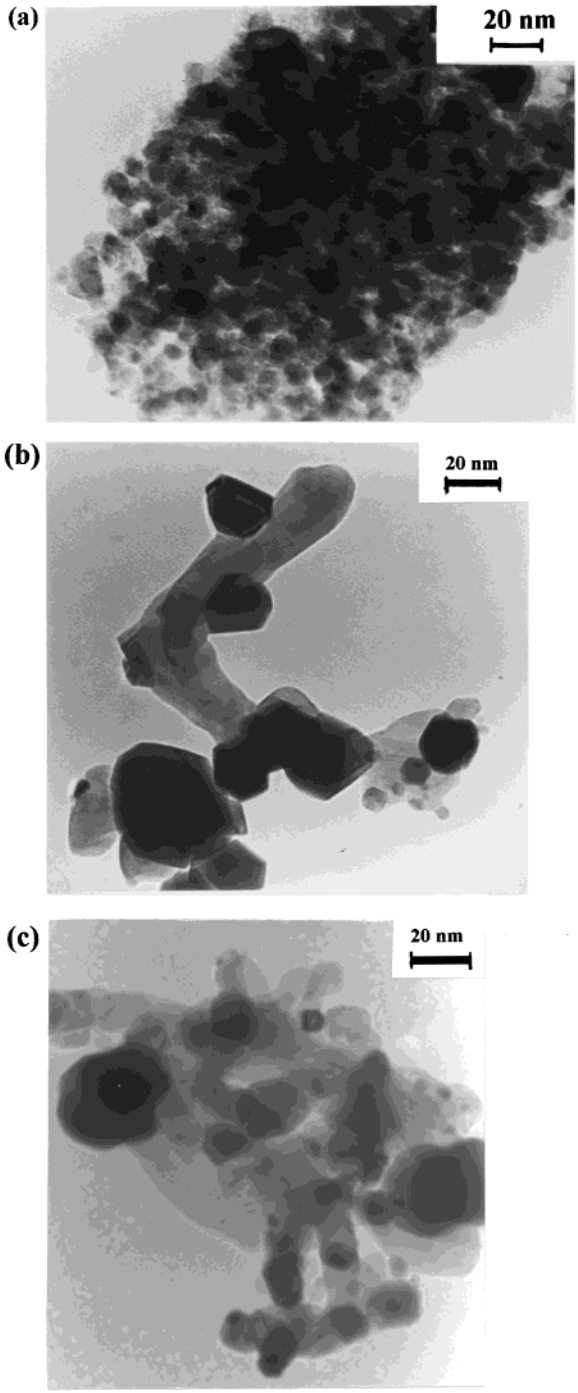

Figure 7. TEM micrographs of (a) SiC/TiC, (b) SiC/NbC, and (c) SiC/TaC ceramics pyrolyzed at 1400 °C for 2h.

polymer cross-linking. In comparison to the DSC curve obtained during the thermal treatment of a TiO_2/**1** dispersion (Figure 9d), the plot obtained for the precursor **2** (Figure 9a) reflects the high degree of entanglement between the components,[27] which is in agreement with the TEM results. MS analyses of the decomposition gases showed predominantly H_2O during the first weight loss (50−250 °C, 15%) and $CH_4 + H_2$ during the second one (400−750 °C, 6%). Finally, there was the major weight loss that took place at temperatures higher than 1150 °C, corresponding to the carbothermal reduction of the metal oxides to the metal carbides (40%). In this temperature domain, only CO is detected by mass spectroscopy. Thermal studies conducted on

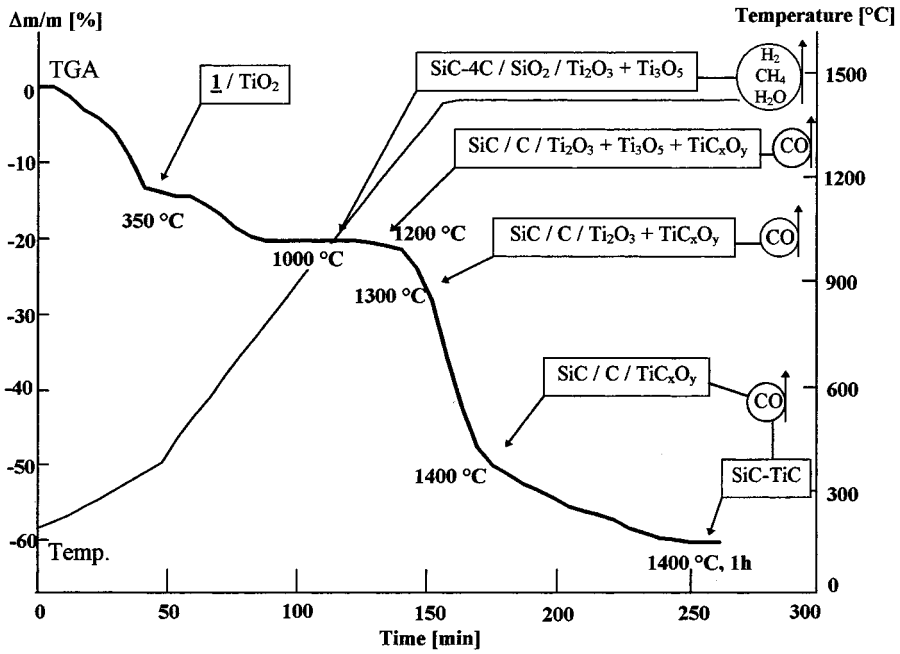

Figure 8. TGA curve of **2**. The crystalline phases, detected by XRD, are given inside rectangles. The off-gases, detected by MS, are given inside circles.

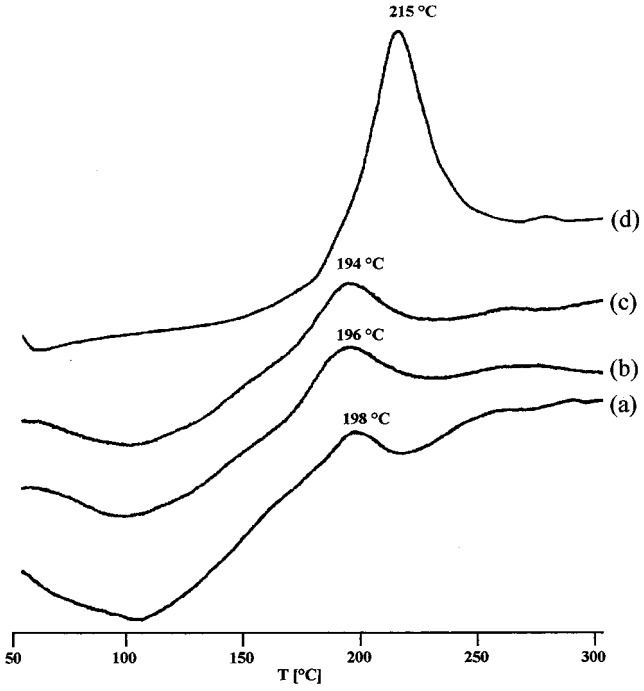

Figure 9. Differential scanning analyses (DSC) of (a) **2**, (b) **3**, (c) **4** and (d) **1**/TiO_2 dispersion.

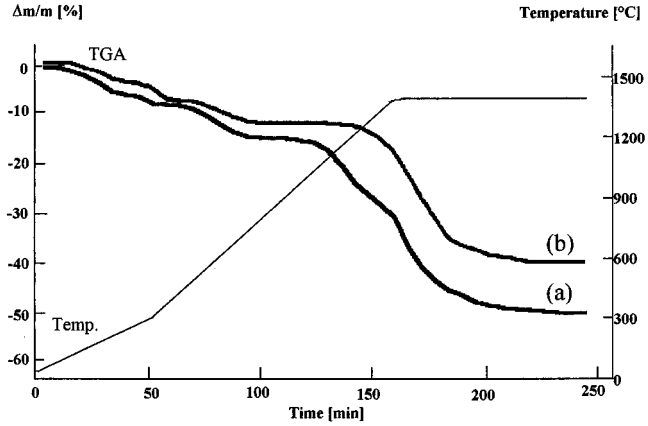

Figure 10. TGA curves of (a) **3** and (b) **4**.

precursors **3** and **4** showed a similar behavior (Figure 10).

The infrared spectroscopy results (Figure 1) also give some evidence concerning the chemical transformations occurring during the first step of pyrolysis (20−350 °C). As the temperature is increased, the decrease of the relative intensity of the strong broad band centered at (3347 cm^{-1}) (OH groups) indicated the dehydration of the inorganic component. Simultaneously, at temperatures above 150 °C, the strong sharp band characteristic of the diacetylenic units (2073 cm^{-1}) decreased in intensity, whereas two new bands appeared (2126, 1850 cm^{-1}). These new vibrations arose from the thermal conversion of the diacetylenic units into an ene−yne network (eq 5).[25,26] Finally, at 350 °C, the infrared spectrum is characteristic of a material formed by a C sp^2−metal oxide matrix bearing $SiMe_2$ groups.

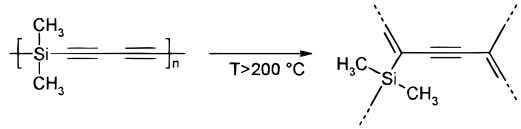

(5)

The ceramic conversion processes were followed by X-ray diffraction techniques. The patterns of the ceramics prepared starting from **2** at different temperatures are shown in Figure 3. When the precursor was heated at 1000 °C for 10 min (Figure 3a), the material was found to be mainly composed of Magneli phases, Ti_3O_5 and Ti_2O_3,[39] of titanium oxycarbide, TiC_xO_y,[39] of β-SiC, and of α-SiO_2. Surprisingly, no peaks corresponding to titanium(IV) oxides are detected; only titanium low oxides were found. This result reflects the reduction of the in situ precipitated TiO_2 by the reductive gases (H_2,

(39) Berger, L. M. *J. Hard Mater.* **1992**, *3*, 3.

CH_4) evolved during the mineralization of the organometallic matrix (vide supra).[40,41] The presence of α-SiO_2 may be related to a reaction between the nascent SiC and titanium oxides, which also resulted in the formation of titanium oxycarbide (eq 6).

$$SiC + 2TiO_2 \rightarrow SiO_2 + 2TiCO \qquad (6)$$

Increasing the temperature led to an improvement of the crystallinity of the material. The complete disappearance of α-SiO_2 at 1200 °C (Figure 3b) indicated that the carbothermal reduction processes induced by the carbon coming from the degradation of **1** started in this temperature range. Finally, the titanium carbide, which was unambiguously observed at 1400 °C, reached its optimal cell parameter after 1 h at this temperature (Figure 3e).

In the case of precursors **3** and **4**, the X-ray diffraction patterns of the ceramics prepared at different temperatures are given in Figures 4 and 5, respectively. As shown in Figure 4a, NbO_2 was formed as the unique crystalline phase at 1000 °C. As observed for **2**, this result indicates the reduction of the intermediate niobium(V) oxides during the earlier stage of the pyrolysis. The onset of NbC crystallization was found at 1200 °C. Upon treatment at 1400 °C for 10 min, NbO_2 completely disappeared for the benefit of NbC. Further heating at this temperature involved an improvement of the crystallinity of the ceramic, allowing a clear observation of *β*-SiC (Figure 4e).

In contrast to the above observations, no intermediate suboxides were observed during the pyrolysis of precursor **4**, *δ*-Ta_2O_5 is the unique oxide phase crystallized at 1000 °C (Figure 5a). Tantalum carbide phases (*ζ*-$TaC_{0.6}$ and TaC), which are also identified at this temperature indicated that the carbothermal reduction process had already taken place. Moreover, on account of their very small crystallite size, the X-ray patterns of the tantalum carbide phases appeared to be very broadened. On heating at higher temperatures, the peaks assigned to the oxide phases gradually decreased and finally disappear after 1 h at 1400 °C (Figure 5e).

(40) Kamiya, K.; Yoko, T.; Bessho, M. *J. Mater. Sci.* **1987**, *22*, 937.
(41) Kohno, K. *J. Mater. Sci.* **1992**, *27*, 658.

Conclusion

We have demonstrated that *β*-SiC/MC (M = Ti, Nb and Ta) nanocomposite ceramics can be prepared by pyrolyses under inert atmosphere of precursors consisting of interpenetrating networks of poly[(dimethylsilylene)diacetylene] **1** and polymeric metal oxides. The precursor-to-ceramic conversion involved two critical transformations. The first one occurred at approximately 200 °C and involved the exothermic cross-linking of the chains of polymer **1** through the polyaddition of the diacetylenic units. The second occurred above 1200 °C and involved the carbothermal reduction of the oxide constituents by the carbon resulting from the degradation of polymer **1**. At 1400 °C, the pure carbides are obtained as nanometer-sized powders. Analyses of the ceramics have shown that we can exclude the existence of solid solutions between *β*-SiC and the other metal carbide. Moreover, EDX analyses showed that the Si/metal ratio was the same as the ratio introduced in the starting material and that this ratio was quite constant for each set of particles throughout the sample. These results indicate that the materials described in this paper can be described as nanocomposite ceramics with interpenetrating networks.

Acknowledgment. The authors thank the CNRS for financial support. We are grateful to Drs. Galy and Baulès (Toulouse, France) for TEM-EDX measurements and fruitful discussions.

CM991140E